Published in Crystal Growth & Design (2011), vol. 11, pp. 1091-1097

cover page

Czochralski crystal growth, thermal conductivity and magnetic properties of $Pr_xLa_{1-x}AlO_3$, where x = 0, 0.75, 0.55, 0.40, 1

S. Turczynski,[†] D. A. Pawlak,[†] R. Diduszko,[†] M. Pękała[§], J. Mucha[‡], J.F. Fagnard[**] , Ph. Vanderbemden[**], M. A. Carpenter[♦]

[†]Institute of Electronic Materials Technology (ITME), ul. Wolczynska 133, 01-919 Warsaw, Poland
[§]Chemistry Dept., Warsaw University, Al. Zwirki i Wigury 101, Pl-02-093, Warsaw, Poland
[‡]Institute of Low Temperature and Structure Research, PAN, 50-950 Wrocław 2, Poland
[**]SUPRATECS, Montefiore Electricity Institute, B28, University of Liege, B-4000 Liege, Belgium
[♦] Department of Earth Sciences, University of Cambridge,Downing Street, Cambridge, CB2 3EQ, U.K.

Corresponding author: Sebastian Turczynski
Institute of Electronic Materials Technology
ul. Wolczynska 133
01-919 Warsaw
Poland
Ph.: +48 22 8349949, +48 22 8353041 ext 175,
E-mail: Sebastian.Turczynski@itme.edu.pl

Abstract. Crystals of $Pr_xLa_{1-x}AlO_3$ solid solution have been grown by the Czochralski method for the first time, to our knowledge. Crystals with high praseodymium concentration tend to grow spirally. The colors of the crystals change with chemical composition. X-ray diffraction shows an increase of the lattice constants with an increase of lanthanum ion concentration. The thermal conductivity has been investigated in the temperature range 5 to 300 K. Completely different behaviour of thermal conductivity is observed at low temperatures for the investigated crystals, while it remains roughly constant at high temperatures. The values of magnetic susceptibility lies within the expected range that could be expect for a paramagnetic material.

Photo of $Pr_{0.55}La_{0.45}AlO_3$ crystal with the iridium wire as a seed and other $Pr_xLa_{1-x}AlO_3$ solid solution crystals grown by the Czochralski method.

Published in Crystal Growth & Design (2011), vol. 11, pp. 1091-1097

Czochralski crystal growth, thermal conductivity and magnetic properties of $Pr_xLa_{1-x}AlO_3$, where x = 0, 0.75, 0.55, 0.40, 1

S. Turczynski,[†] D. A. Pawlak,[†] R. Diduszko,[†] J. Mucha[‡], M. Pękała[§], J.F. Fagnard[**], Ph. Vanderbemden[**], M. A. Carpenter[♦]*

Institute of Electronic Materials Technology (ITME), ul. Wolczynska 133, 01-919 Warsaw, Poland, Institute of Low Temperature and Structure Research, PAN, 50-950 Wrocław 2, Poland, Chemistry Dept., Warsaw University, Al. Zwirki i Wigury 101, Pl-02-093, Warsaw, Poland, SUPRATECS, Montefiore Electricity Institute, B28, University of Liege, B-4000 Liege, Belgium

Department of Earth Sciences, University of Cambridge,Downing Street, Cambridge, CB2 3EQ, U.K

E-mail: Sebastian.Turczynski@itme.edu.pl

RECEIVED DATE

Abstract. Crystals of $Pr_xLa_{1-x}AlO_3$ solid solution have been grown by the Czochralski method for the first time, to our knowledge. Crystals with high praseodymium concentration tend to grow spirally. The color of the crystals changes with chemical composition. X-ray diffraction shows an increase of the lattice constants with an increase of lanthanum ion concentration. The thermal conductivity has been investigated in the temperature range 5 to 300 K. Completely different behaviour of thermal conductivity is observed at low temperatures for the investigated crystals, while it remains roughly constant at high temperatures. The values of magnetic susceptibility lies within the expected range that could be expect for a paramagnetic material.

Keywords: $PrAlO_3$, $LaAlO_3$, $Pr_xLa_{1-x}AlO_3$, perovskites, single crystal growth, Czochralski method.

[*] Corresponding author. E-mail:Sebastian.Turczynski@itme.edu.pl Telephone: +48 22 8349949
[†] Institute of Electronic Materials Technology
[‡] Institute of Low Temperature and Structure Research
[§] Chemistry Dept., Warsaw University
[**] Montefiore Electricity Institute
[♦] Department of Earth Sciences,

Introduction

$LaAlO_3$ has a phase transition from high-temperature cubic phase to low-temperature rhombohedral phase at 833K which will generate micro-twins, ferroelastic domains, a rough surface and lateral distortions.[1] $PrAlO_3$ is likewise a rhombohedrally-distorted perovskite (space group $R\bar{3}c$, tilt system $\overline{aaa}$) at room temperature[2, 3, 4]. The distortion from cubic symmetry is associated with the tilting of the AlO_6 octahedra about the three-fold axis, and this is progressively reduced as the temperature is increased above room temperature, until at 1864 K, $PrAlO_3$ transforms to the cubic structure of the ideal perovskite[5, 6, 19]. The transition temperature is between that of $LaAlO_3$ (transition at 833K) and that of $NdAlO_3$ (transition at ca. 2200K). Microtwins are also observed in $PrAlO_3$ crystals[7, 8]. $PrAlO_3$ differs from $LaAlO_3$ and $NdAlO_3$ in that it undergoes further phase transitions below room temperature[9, 10, 11, 12, 13, 14, 15]: a first-order transition at about 205 K and a continuous transition near 150K. The phase transitions of $PrAlO_3$ can be described as: $C2/m \xrightarrow[150K]{} Imma \xrightarrow[205K]{} R\bar{3}c \xrightarrow[1864\pm31K]{} Pm\bar{3}m$.[4, 5, 6, 16, 17, 18, 19]. The change of $PrAlO_3$ structure with pressure has been also recently investigated[18, 20]. The additional transitions below room temperature are ascribed to the so-called ion lattice coupling. Harley et al.[11] state that the Pr^{3+} ion in its ground state favors a tetragonal distortion, whereas elastic forces favor a trigonal distortion. Competition between these competing requirements causes the observed sequence of transitions[11, 12].

Phase transitions in $Pr_xLa_{1-x}AlO_3$ solid solution perovskites were first investigated in 1970's. Samples were obtained by different methods, such as the flux growth method[11, 21]. Polycrystalline samples were prepared using conventional solid-state method[16, 18]. Physical properties of $Pr_xLa_{1-x}AlO_3$ were determined by: neutron powder diffraction[4], EPR[11], Raman spectroscopy[11, 21], low temperature XRD[16] and high-pressure powder synchrotron X-ray diffraction[18]. High-temperature phase transitions were detected in $Pr_xLa_{1-x}AlO_3$, with the temperatures decreasing with increasing lanthanum content. Low-temperature phase transitions were detected only in crystals with x = 0.2-0.66[15]. The mechanisms of the high and low-phase transitions are different. Below room temperature $Pr_xLa_{1-x}AlO_3$ perovskites

show interesting structural behavior. High-temperature transitions are caused by octahedral tilting within the perovskite structure, while the low-temperature transitions are caused by electronic effects[15].

No data on single crystal growth of $Pr_xLa_{1-x}AlO_3$ could be found. Wanklyn et al. prepared millimeter-sized samples of $PrAlO_3$ and other rare earth aluminates by the flux method[22], while Pawlak et al. prepared the $PrAlO_3$ crystals by the Czochralski method[7]. Novoselov presented $PrAlO_3$ crystals doped with Ce and Sr, grown by the micro-pulling down method[23, 24]. The melting temperature of $PrAlO_3$ was quoted as ca. 2350K [15].

$Pr_xLa_{1-x}AlO_3$ has attracted a lot of attention due to its many phase transitions and the change of electronic, magnetic and structural properties. By changing the Pr:La ratio in $Pr_xLa_{1-x}AlO_3$ single crystals the phase transitions can be engineered. In this work we describe the growth of $Pr_xLa_{1-x}AlO_3$ bulk single crystals by the Czochralski method, where x = 0, 0.75, 0.55, 0.40, 1. Structural and magnetic properties as well as thermal conductivity for $Pr_xLa_{1-x}AlO_3$, where x = 0, 0.55, 1 are also presented and discussed here.

Experimental

Crystal growth. $Pr_xLa_{1-x}AlO_3$ crystals, where x=1, 0.75, 0.55, 0.4, 0, have been obtained using the Czochralski method[25]. The melts were prepared from high purity Pr_6O_{11}, Al_2O_3 and La_2O_3 oxides (99,995%). All components were mixed in stoichiometric ratios. A conventional Czochralski apparatus, Oxypuller 05–03 (Cyberstar), and RF heating were used. The crystals were grown from an iridium crucible, 50 mm in height and diameter. The pulling and rotation rates were 1-1,7mm/h and 6-8rpm, respectively. The crystals were seeded-grown with iridium wires (Fig. 1). The crystals were about 20mm in diameter and 50mm in length. A pure nitrogen atmosphere was applied. This is in contrast to the single crystals obtained by Pawlak et al. which were obtained in partially oxidizing atmosphere (ca. 20÷30ppm)[7].

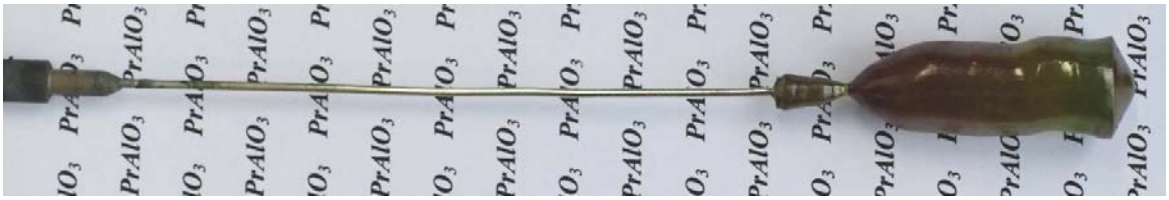

Figure 1. $Pr_{0.55}La_{0.45}AlO_3$ crystal with the iridium wire-seed, grown by the Czochralski method.

XRD analyses. In order to confirm the structural state of as-grown $Pr_xLa_{1-x}AlO_3$ crystals, powder X-ray Diffraction experiments have been performed. The XRD data were collected on a Siemens D500 diffractometer equipped with semiconductor Si:Li detector and $K_\alpha Cu$ radiation. Intensity of the diffraction peaks was recorded in the range of $2\theta=15^o–82^o$ with a step size of 0.02^o and an integration time of 10 s/step.

Magnetic susceptibility. The temperature dependence of the AC magnetic susceptibility was measured at 1 mT amplitude. The temperature variation of the field-cooled (FC) and zero-field-cooled (ZFC) DC magnetization was recorded under an applied DC field $\mu 0H$ of 10 mT. More details have been described elsewhere [26, 27].

Thermal conductivity. The thermal conductivity was measured using the stationary heat flux method in the temperature range 5 – 300 K. The experimental setup and the measurement procedure have been described in detail in[28, 29]. The temperature gradient along the sample was in the range 0.1 – 0.5 K. Particular care was taken to avoid a parasitic heat transfer between the sample and its environment. The measurement error was below 2% and the surplus error estimated from the scatter in the measurement points did not exceed 0.3%.

Results and Discussion

Structural results. Data for $Pr_xLa_{1-x}AlO_3$ crystals, where x=1, 0.75, 0.55, 0.4, 0, are given in Tab. 1. The crystals themselves are shown in Fig. 2. The crystal compositions measured with inductive coupled plasma optical emission spectroscopy (ICP-OES) differ slightly from the raw materials compositions.

The determined concentration of Pr ions is lower, and of La ions is higher than the nominal values (Tab. 1). A tendency to grow with slight spirality at the ends has been observed in the crystals with high praseodymium concentration. This was not observed in the $LaAlO_3$ crystal. The colors of the crystals have different origins: the dark brown colour is probably a result of the presence of Pr^{4+} ions[7, 30, 31], while the light green colour is typical for Pr^{3+} ions[7, 30, 31]. The brownish-red coloration mostly in the $LaAlO_3$ crystal is probably due to the colour centres[32, 33].

Table 1. Chemical composition and crystallographic data of $Pr_xLa_{1-x}AlO_3$ crystals.

Crystal	Stoichiometric composition	Measured chemical composition[a]	Crystallographic data in rhombohedral and hexagonal notation
a	$PrAlO_3$	$Pr_{0.9893}AlO_{3.0873}$	a_r=5,309Å; α=60,24º | a_h=5,3325Å; c=12,969Å; V=319,38Å^3
b	$PrAlO_3$	-----	a_r=5,313Å; α=59,91º | a_h=5,3322Å; c=12,968Å; V=319,32Å^3
c	$Pr_{0.75}La_{0.25}AlO_3$	$Pr_{0.725}La_{0.275}AlO_3$	a_r=5,332Å; α=60,12º | a_h=5,3414Å; c=13,006Å; V=321,35Å^3
d	$Pr_{0.55}La_{0.45}AlO_3$	$Pr_{0.514}La_{0.486}AlO_3$	a_r=5,325Å; α=59,89º | a_h=5,3467Å; c=13,036Å; V=322,74Å^3
e	$Pr_{0.40}La_{0.60}AlO_3$	$Pr_{0.364}La_{0.636}AlO_3$	a_r=5,336Å; α=60,01º | a_h=5,3526Å; c=13,060Å; V=324,05Å^3
f	$LaAlO_3$	$La_{1.0007}AlO_{3.0066}$	a_r=5,352Å; α=60,00º | a_h=5,3598Å; c=13,097Å; V=325,84Å^3

[a] *Chemical composition investigated by ICP-OES*

From powder X-ray diffraction we can conclude that all the crystals consisted of one phase, with the rhombohedral perovskite structure (Fig. 3). The XRD analysis also indicates that $Pr_xLa_{1-x}AlO_3$ crystals all solidify in a rhombohedral structure. The observed reflections are consistent with $R\bar{3}c$ space group. Lattice constant of the $PrAlO_3$ crystal, a_h =5.3325, c_h = 12.969 Å (for the first crystal) and a_h =5.3322, c_h = 12.968 Å (for the second crystal) are in agreement with the reference values given in hexagonal notation (a_h =5.3328, c_h = 12.973 Å[7] and a_h =5.332, c_h = 12.97 Å[34]). The measured lattice constant of the $LaAlO_3$, a_h=5,3598Å; c=13,097Å, are also in agreement with the literature data (a_h=5,3653Å; c=13,112 Å)[35].

Figure 2. A series of $Pr_xLa_{1-x}AlO_3$ crystals grown by the Czochralski method: a) x=1, b) x=1, c) x=0.75, d) x=0.55, e) x=0.4, f) x=0.

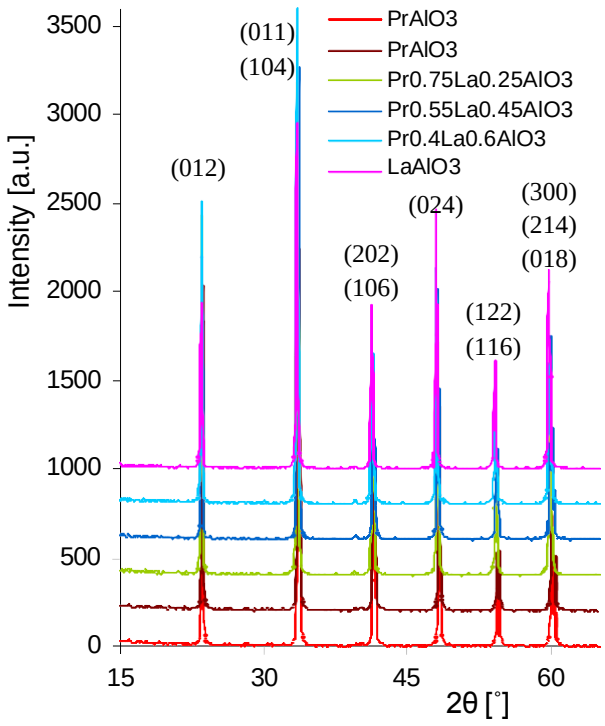

Figure 3. Powder X-ray diffraction peaks of $Pr_xLa_{1-x}AlO_3$ indicate one-phase for all obtained crystals.

Lattice parameters for all as-grown crystals in both rhombohedral and hexagonal notation are shown in Table 1. Diffraction peaks at higher values of 2θ show a continuous shift towards lower 2θ angles with increasing amount of lanthanum ions substituting for praseodymium (Fig. 4). This is connected with an increase of the lattice parameters of $Pr_xLa_{1-x}AlO_3$ crystals with increasing concentration of lanthanum ions (La^{3+}_{IX}=1,216), which have bigger ionic radii than praseodymium ions (Pr^{3+}_{IX}=1,179)[36]. Figure 5 shows the impact of increasing La ion concentration on lattice parameters in agreement with Vegard's law. Apart from changes of the lattice parameters, the angle in rhombohedral notation for the $LaAlO_3$ crystal is much closer to 60° than for $PrAlO_3$. This indicates that the distortion from a cubic lattice is smallest in $LaAlO_3$ crystal.

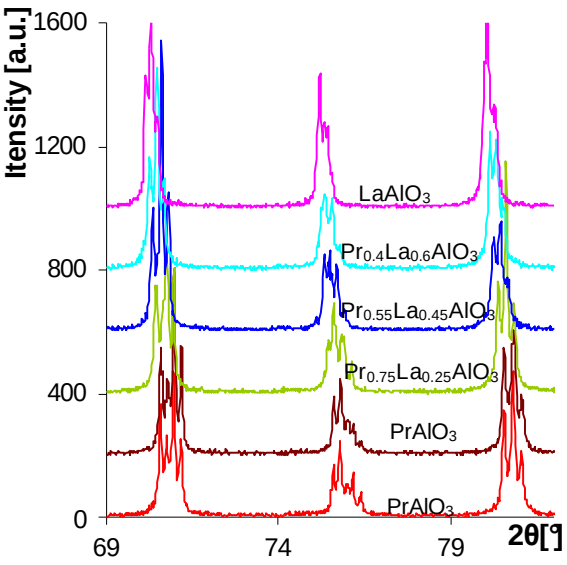

Figure 4. Powder X-ray diffraction peaks of $Pr_xLa_{1-x}AlO_3$ crystals. The peaks shift to lower 2θ values with higher concentration of lanthanum ions.

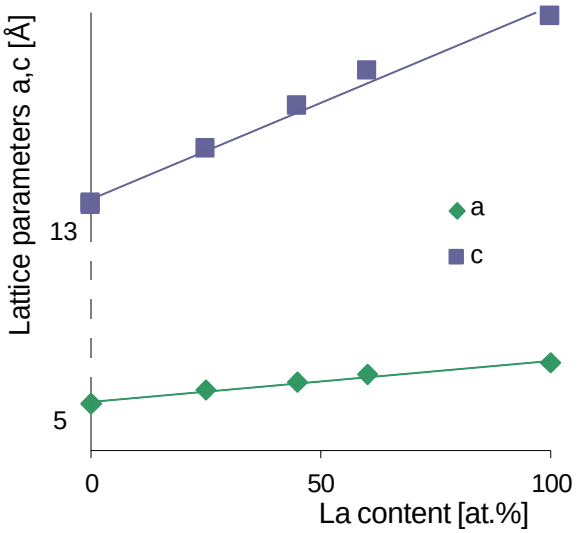

Figure 5. Dependence of 'a' and 'c' lattice parameters of $Pr_xLa_{1-x}AlO_3$ crystals on the La ions concentration.

Magnetic characterization. The magnetic properties of $Pr_xLa_{1-x}AlO_3$ crystals, where x=0, 0.55, 1, have been investigated. The values of magnetic susceptibility lies within the expected range that could be expect for a paramagnetic material (Fig. 6). The magnetic susceptibility of two samples containing Pr atoms is approximately four times larger than for $LaAlO_3$ sample. The almost temperature-independent behavior found in $LaAlO_3$ most probably resembles so-called **van Vleck paramagnetism**[9]. All three susceptibility curves exhibit a maximum at around 160 – 180K, which is followed by a very similar curvature between 180 and 210K. One may notice that the observed magnetic susceptibility maximum is located close to the second-order phase transition reported in $PrAlO_3$ at 151K[9, 31, 37]. Moreover, the susceptibility variation of the three samples above 290K is very similar. These features suggest treating the $LaAlO_3$ as a reference and decomposing the measured magnetic susceptibility into the van Vleck component related to $LaAlO_3$, $\chi_{Al}(T)$, and the susceptibility component for Pr atoms, $\chi_{Pr}(T)$, respectively. Thus, the susceptibility components have been analysed according to:

$$\chi(T) = \chi_{Al}(T) + \chi_{Pr}(T)$$

The inverse susceptibilities ($1/\chi_{Pr}(T)$) are plotted for $PrAlO_3$ and $Pr_{.55}La_{.45}AlO_3$ systems in Fig. 6b. In the $R\bar{3}c$ phase appearing above 210K [6] two temperature intervals (from 210 to 290K, and above 290K) may be distinguished, which as a first approximation can be described using the Curie – Weiss expression:

$$\chi_{Pr}(T) = C / (T – T_W),$$

where C and T_W stand for the Curie constant and the Weiss temperature, respectively.

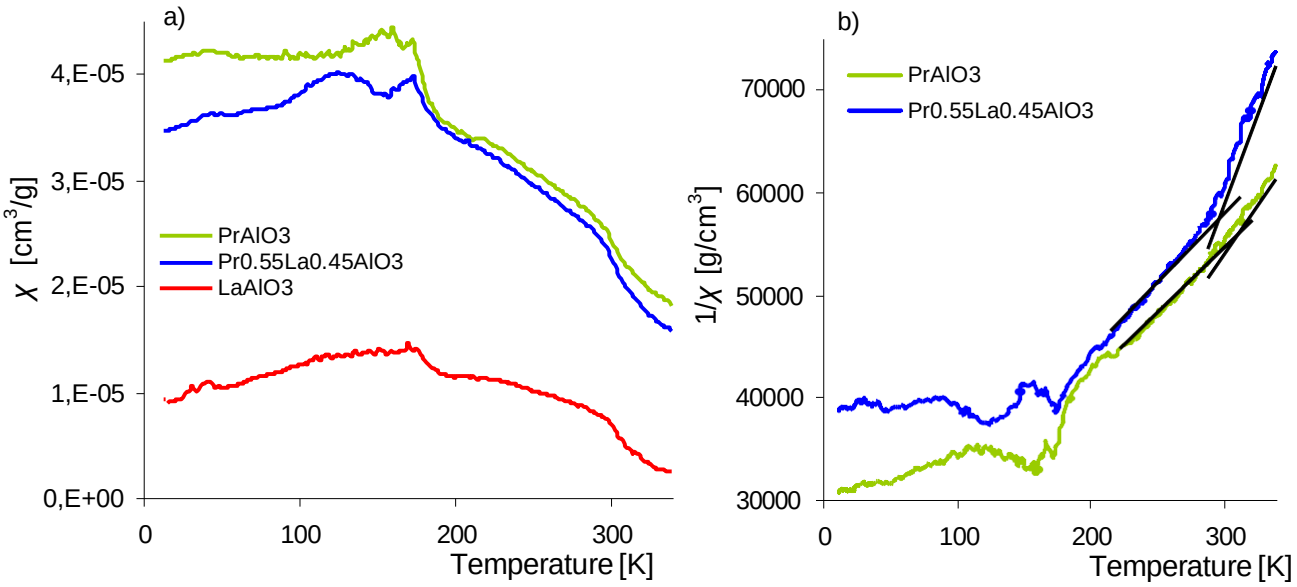

Figure 6. Magnetic properties of $PrAlO_3$, $Pr_{0.55}La_{0.45}AlO_3$ and $LaAlO_3$ crystals. (a) susceptibility dependence on temperature $\chi(T)$, (b) temperature dependence of the inverse susceptibility $1/\chi(T)$. The magnetic susceptibility was measured in magnetic fields below 1 Oe. Straight lines show a fit to the Curie - Weiss law below and above 290 K.

The parameters derived by a fitting to a Curie – Weiss law (Tab. 2) reveal a remarkable changeover occurring at about 290K. As the temperature intervals are relatively narrow, values of the effective magnetic moments are determined with accuracy of about 2% and 7 % for temperatures below and above 290K, respectively. It is noteworthy that the effective magnetic moment per Pr^{3+} ion (see Tab. 2) is higher below 290K for both the $PrAlO_3$ and $Pr_{0.55}La_{0.45}AlO_3$ systems. Moreover, the magnetic moments below 290K, are much higher than the expected free ion Pr^{3+} value of $3.6\mu_B$. The applied numerical separation of the van Vleck and Curie-Weiss susceptibility components shows that these components cannot be entirely responsible for the huge values of effective magnetic moments found below 290K, even assuming the overestimated 10% inaccuracy of the van Vleck component. This could indicate that the susceptibility separation is too crude in this case, or some additional mechanisms such as the formation of a superparamagnetic phase and/or crystal field effects may be important.

In the first scenario the superparamagnetic phase with a large magnetic moment composed of many atoms contained in a grain or cluster often appears in the vicinity of the paramagnetic Curie temperature. For both the Pr containing samples it is revealed by a lower slope in the temperature dependence of the inverse susceptibility below 290 K as compared to the higher temperatures. According to structural data one may suppose that the superparamagnetic grains are preferentially formed within the planes of Pr/Al atoms. The distance between these atoms are as low as 0.5312 nm and the Pr-O-Pr angle is 180°, which may facilitate a stronger exchange interaction leading to superparamagnetism. The exchange interaction may also be enhanced due to local lattice deformations and strains.

Tab. 2. Effective magnetic moment and Weiss temperature derived from Curie - Weiss law for $PrAlO_3$ and $Pr_{0.55}La_{0.45}AlO_3$ crystals.

Sample	Temperature interval {K}	Effective magnetic moment (μ_B)	T_W = Weiss temperature (K)
$Pr_{0.55}La_{0.45}AlO_3$	210-290	3.92/7.13*	-80
$Pr_{0.55}La_{0.45}AlO_3$	290-340	1.87/3.4*	113
$PrAlO_3$	210-290	4.86	-133
$PrAlO_3$	290-340	3.48	-14

* The smaller value is per $Pr_{0.55}La_{0.45}AlO_3$, the higher value is per Pr^{3+} ion

It is well known that the higher multiplets in praseodymium are located very close to the ground one. This can make the magnetic moment of Pr^{3+} more dependent on crystal field effects [31]. Such additional contributions are not taken into account when the classical Curie–Weiss is derived, since this assumes only the ground state is occupied, and there is no magnetic anisotropy[38]. A more advanced susceptibility analysis is presently not possible, since the magnetic susceptibility of $PrAlO_3$ and $Pr_{0.55}La_{0.45}AlO_3$ systems was measured within the (001) and (110) crystallographic planes, respectively. Therefore, the measured susceptibility is an average of the components along the principal axes. These susceptibility

components and the relation to magnetic and structural anisotropy will be studied in more detail, if well- oriented crystals will become available.

For $PrAlO_3$ the negative Weiss temperature T_W values of -133 and -14K derived from the 210-290 and 290-340 K intervals, respectively, indicate the average antiferromagnetic interaction between the Pr^{3+} magnetic moments. These values are not very different from the -52K reported for T > 205K[9]. The $Pr_{0.55}La_{0.45}AlO_3$ system has the more complex behavior, since T_W = -80K for the 210-290K interval changes to T_W = 113K at higher temperatures. The sign change in T_W points to an average ferromagnetic interaction in the temperature range above 290K. The sign change in T_W occurs close to the irreversibility temperature T_{IR}=310K, where the zero (ZFC) and field (FC) cooled curves start to diverge (Fig. 7). On the other hand, in $PrAlO_3$, where a tendency to ferromagnetic ordering is relatively weak, the irreversibility effects appear below T_{IR} = 290K. The irreversibility processes may be caused by the magnetic anisotropy and/or the phase separation on twin boundaries [39]. There is also an abrupt increase in magnetization above T_{IR} for both systems containing Pr. Such behavior may reveal weakly ferromagnetic ordering of Pr^{3+} ions. The high temperature magnetization increase is larger for the $Pr_{0.55}La_{0.45}AlO_3$ exhibiting the positive T_W value. The puzzling behavior of ZFC and FC magnetization in $LaAlO_3$ cannot be fully explained without more detailed studies.

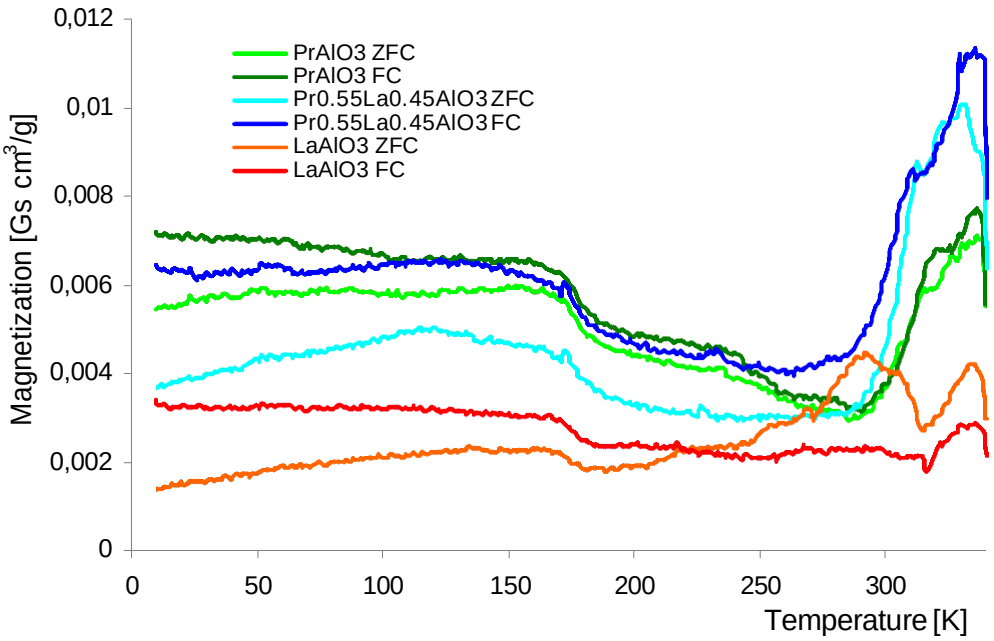

Figure 7. The dependence of ZFC and FC magnetization on temperature, *M(T)* for $PrAlO_3$, $Pr_{0.55}La_{0.45}AlO_3$ and $LaAlO_3$ crystals. The temperature variation of the field-cooled (FC) and zero-field-cooled (ZFC) DC magnetization was recorded under an applied DC field μ0H of 10 mT.

Thermal Conductivity. Thermal conductivities of $PrAlO_3$, $Pr_{0.55}La_{0.45}AlO_3$, $LaAlO_3$ are presented in Fig. 8, in the temperature range 5-300K. All samples are very good insulators, so heat transfer can be attributed to phonons. At high temperatures, thermal conductivities (κ) for all samples are close to 6W/Km. At low temperatures large differences can be seen both in the values of the thermal conductivity and their temperature dependences. The maximum of *κ(T)* occurs at 30K for $PrAlO_3$ and at 40K for $Pr_{0.55}La_{0.45}AlO_3$, and such behavior is characteristic for dielectrics. However for $LaAlO_3$ a broad maximum is observed only at 135K – which is typical for some non-magnetic compounds with Lu, La and Y. Above the temperature of the thermal conductivity maximum *κ(T)* is a decreasing function, Fig. 8a. Moreover some small minima in the thermal conductivity can be observed at 150K and 120K for $PrAlO_3$ and $Pr_{0.55}La_{0.45}AlO_3$, respectively. In the case of $PrAlO_3$, this may be connected with the phase transition at 151K. For $Pr_xLa_{1-x}AlO_3$ crystals this phase transition will take place at lower temperature depending on the concentration of praseodymium ions (Pr concentration↓ temp. of the

phase transition↓)[15], so we can assume that the observed minimum at 120K for $Pr_{0.55}La_{0.45}AlO_3$ is due to the phase transition. Thermal conductivity can be given by the following kinetic formula: $\kappa(T) = 1/3Cv\ell$, where C is heat capacity of the lattice, v is average phonon velocity and ℓ is average free path of phonons. The temperature dependences of the *C*, υ and l determine $\kappa(T)$. Fig. 8b shows the temperature dependences of thermal conductivity on a log-log scale. At low temperatures the thermal conductivity of $LaAlO_3$ and $Pr_{0.55}La_{0.45}AlO_3$ varies with temperature as T^1 and as $T^{0.7}$, respectively. This is connected with the dispersion of phonons on the point defects, especially for $Pr_{0.55}La_{0.45}AlO_3$. At T* = 16 K a significant change of temperature dependence of $\kappa(T)$ can be seen: T^1 for $Pr_{0.55}La_{0.45}AlO_3$ and $T^{0.9}$ for $LaAlO_3$. This change of phonon-defect interaction is probably associated with the phase transition, which causes the number and kind of defects in the crystal lattice to change. The temperature dependence of the thermal conductivity for $PrAlO_3$ crystal is completely different. The thermal conductivity for this crystal varies as $T^{2.3}$. This could be connected with dispersion of phonons on the microtwin boundaries in addition to the phonon-defect dispersion existing in other crystals. At temperatures above the maximum temperature of the thermal conductivity, the thermal resistance (κ^{-1}) depends mainly on phonon-phonon and phonon-defect interaction (such as dislocations). The thermal conductivity for $PrAlO_3$, $LaAlO_3$ and $Pr_{0.55}La_{0.45}AlO_3$ changes as $T^{-2.2}$, $T^{-0.1}$ and $T^{-1.1}$, respectively. Minima in $\kappa(T)$ are observed at 150 and 120 K for $PrAlO_3$ and $LaAlO_3$, respectively, while a small maximum is observed for $LaAlO_3$ at 120K. Comparing temperature dependences of the thermal conductivity for $PrAlO_3$ and $Pr_{0.55}La_{0.45}AlO_3$, a strong influence of praseodymium ions concentration on $\kappa(T)$ can be seen. The explanation may be as follows: in $PrAlO_3$ there is a second-order phase transition at 150K, during which the lattice constants change. The change of the lattice constants may strongly influence thermal conductivity.

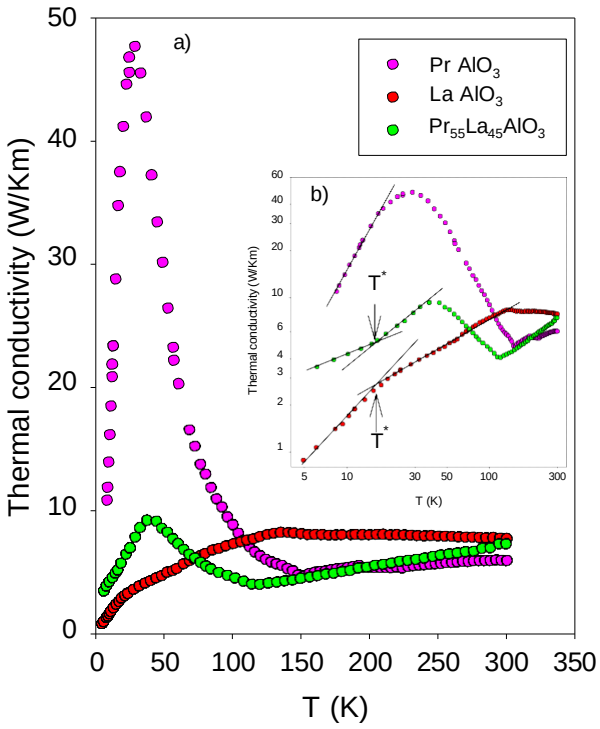

Figure 8. Thermal conductivity of $PrAlO_3$, $Pr_{0.55}La_{0.45}AlO_3$, $LaAlO_3$ crystals in the temperature range from 5 to 300K.

Conclusions

$Pr_xLa_{1-x}AlO_3$ crystals, where x=1, 0.75, 0.55, 0.4, 0, have been grown by the Czochralski method. The crystals had the following compositions $Pr_{0.9893}AlO_{30873}$, $Pr_{0.725}La_{0.275}AlO_{3.0504}$, $Pr_{0.514}La_{0.486}AlO_{2.8647}$, $Pr_{0.364}La_{0.636}AlO_{3.0003}$, and $La_{1.0007}AlO_{3.0066}$ as investigated by ICP OES. Due to the phase transition between the melting temperature and the room temperature the crystals had to be seeded-grown with iridium wires. Crystals with high praseodymium content had a tendency to grow spirally. X-ray diffraction analysis shows that $LaAlO_3$ is much less distorted from a cubic system than $PrAlO_3$, and that the lattice parameters in $Pr_xLa_{1-x}AlO_3$ crystals increase with increasing lanthanum concentration. The values of magnetic susceptibility lies within the expected range that could be expect for a paramagnetic material. Numerical separation of the van Vleck and Curie-Weiss susceptibility components shows that these components cannot be entirely responsible for the huge values of effective magnetic moments found below 290K, even assuming the overestimated 10% inaccuracy of the van Vleck contribution.

The thermal conductivity has been measured for $PrAlO_3$, $Pr_{0.55}La_{0.45}AlO_3$, and $LaAlO_3$ crystals in the temperature range from 5 to 300 K. At higher temperatures the thermal conductivity of all investigated crystals is similar, while at lower temperatures there are considerable differences. Changes in the temperature dependence of thermal conductivity are seen at the temperatures of the second-order transition for $PrAlO_3$ at 151 K and for $Pr_{0.55}La_{0.45}AlO_3$ at 120K.

Acknowledgments. The authors thank the FP7 NMP ENSEMBLE Project (GA NMP4-SL-2008-213669) and the Ministry of Science and Higher Education of Poland for support (Grant No. N 5076 143 32/4056) for partially supporting this work. This work has been partially supported by Ministry of Science and Higher Education (Poland - Wallony). The authors thank to Marek Swirkowicz, Tadeusz Telak, Dariusz Artel and Wlodek Szyrski from ITME for help with crystal growth processes. Authors are grateful to Dr. hab. A. Szewczyk for fruitful discussions.

References

(1) M.M.C. Chou, Ch. Chen, S.S. Yang, Ch.H. Huang, H.L. Huang, *J. of Phys. Chem. Solids* **2008**, *69*, 425.

(2) A.M. Glazer, *Acta Cryst.* **1972**, *B28* 3384.

(3) A.M. Glazer, *Acta Cryst*. **1975**, *A31*, 3384.

(4) C.J. Howard, B.J. Kennedy, B.C. Chakoumakos, *J. Phys. Condens. Matter*. **2000**, *12*, 349.

(5) C.J. Howard, H. Stokes, *Acta Cryst.* **1998**, *B54*, 782.

(6) M.A. Carpenter, C.J. Howard, B.J. Kenned, K.S. Knight, *Phys. Rev. B* **2005**, *72*, 024118.

(7) D.A. Pawlak, T. Lukasiewicz, M. Carpenter, M. Malinowski, R. Diduszko, J. Kisielewski, *J. Cryst. Growth* **2005**, *282*, 260-269.

(8) K. Wieteska, W. Wierzchowski, A. Malinowska, S. Turczynski, M. Lefeld-Sosnowska, D. A. Pawlak, T. Lukasiewicz, W. Graeff, 2010 – submitted to Acta Physica Polonica.

(9) E. Cohen, L.A. Risberg, W.A. Nordland, R.D. Burbank, R.C. Sherwood, L.G. Van Uitert, Phys. Rev. **1969**, *186*, 476.

(10) R.D. Burbank, *J. Appl. Cryst*. **1970**, *3*, 112.

(11) R.T. Harley, W. Hayes, A.M. Perry, S.R.P. Smith, *J. Phys*. **1973**, *C6*, 2382.

(12) R.J. Birgeneau, J.K. Kjems, G. Shirane, L.G. Van Uitert, *Phys. Rev*. **1974**, *B10*, 2512.

(13) K.B. Lyons, R.J. Birgeneau, E.I. Blount, L.G. Van Uitert, *Phys. Rev*. 1975, *B11*, 891.

(14) J.K. Kjems, G. Shirane, R.J. Birgeneau, L.G. Van Uitert, *Phys. Rev. Lett.* **1973**, *31*,1300.

(15) T. Basyuk, L. Vasylechko, S. Fadeev, I.I. Syvorotka, D. Trots, R. Niewa, *Radiation Phys. Chem.* **2009**, *78*, S97-S100.

(16) S.M. Moussa, B.J. Kennedy, B.A. Hunter, C.J. Howard,T. Vogt, *J. Phys. Condens. Matter* **2001**, *13*, L203.

(17) B.J. Kennedy, A.K. Prodjostanoso, C.J. Howard, *J. Phys. Condens. Matter.* **1999**, *11*, 6319.

(18) B.J. Kennedy, T. Vogt, C.D. Martin, J.B. Parise, J.A.Hriljac, Chem. Mater. 14 (2002) 2644.

(19) M.A. Carpenter, E.C. Wiltshire, C.J. Howard, R.I. Thomson, S. Turczynski, D.A. Pawlak, T. Lukasiewicz, *submitted to Phase Transitions 2010*

(20) J. Zhao, N. L. Ross, R. J. Angel, M. A. Carpenter, Ch. J.Howard, D.A. Pawlak, T. Lukasiewicz, *J. Physics, Condensed Matter*, **2009**, *21*, 235403.

(21) T.J. Glyn, R.T. Harley, W. Hayes, A.J. Rushworth, S.H. Smith, *J. Phys. C: Solid State Phys*. **1975**, *8*, L126-L128.

(22) B.M. Wanklyn, D. Midgley, B.K. Tanner, *J. Cryst. Growth* **1975**, *29*, 281

(23) A. Novoselov, A. Yoshikawa, J. Pejchal, M. Nikl, T. Fukuda, *Optical Materials* **2007**, *30*, 168-170.

(24) A. Novoselov, A. Yoshikawa, N. Solovieva, M. Nikl, *Crystal Research and Technology* **2007**, *42*, 1320-1323

(25) J. Czochralski, *Z. Psych. Chem*. **1918**, *92*, 219.

(26) M. Pekala, V. Drozd, J. F. Fagnard, Ph. Vanderbemden, and M. Ausloos, *J. Appl. Phys*. **2009**, *105*, 013923

(27) F. Wolff Fabris, M. Pekala, V. Drozd, J-F. Fagnard, Ph. Vanderbemden, Ru-Shi Liu, and M. Ausloos, *J. Appl. Phys*. **2007**, *101*, 103904

(28) A. Jeżowski, J. Mucha, G. Pompe, *J. Phys. D: Appl. Phys.* **1987**, *20*, 1500.

(29) J. Mucha, S. Dorbolo, H. Bougrine, K. Durczewski, and M. Ausloos, *Cryogenics* **2000**, *44*, 145

(30) D.A. Pawlak, Z. Frukacz, Z. Mierczyk, A. Suchocki, J. Zachara, *J. Alloys and Comp.* **1998**, *275*, 361.

(31) B. Andrzejewski, D. A. Pawlak, T. Klimczuk, S. Turczynski, *submitted to Chem. Mat.* **2009**.

(32) D.A. Pawlak, M. Ito, L. Dobrzycki, K. Wozniak, M. Oku, K. Shimamura, T. Fukuda, *J. Mat. Res.* **2005**, *20*, 412

(33) Y.C. Chang, De-Sen Hou, Y.D. Yu, S.S. Xie, T. Zhou, *J. Cryst. Growth* **1993**, 1*29, 362*.

(34) JCPS 29-0076.

(35) H. Lehnert, H. Boysen, P. Dreier, Y. Yu, *Zeitschrift fuer Kristallographie* **2000**, *215*, 145.

(36) R.D. Shannon, *Acta Cryst.* **1976**, *A32*, 751.

(37) M. Wencka, S. Vrtnik, M. Jagodič, Z. Jagličić, S. Turczynski, D.A. Pawlak, J. Dolinšek, *Phys. Rev. B*, **2009**, *80*, 224410.

(38) K. Andres, S. Darack, H.R. Ott, *Phys. Rev.* 1979, *B19*, 5475

(39) R. Szymczak, M. Czepelak, R. Kolano, A. Kolano-Burian, B. Krzymańska, H. Szymczak, *J. Mater. Sci.* **2008**, *43*, 1734.